



HAL
open science

A refined sine finite element with transverse normal stress for thermoelastic analysis of laminated composite in cylindrical bending

P. Vidal, O. Polit

► **To cite this version:**

P. Vidal, O. Polit. A refined sine finite element with transverse normal stress for thermoelastic analysis of laminated composite in cylindrical bending. *Journal of Thermal Stresses*, 2011, 34 (11), pp.1185-1204. hal-01366931

HAL Id: hal-01366931

<https://hal.science/hal-01366931>

Submitted on 5 Jan 2018

HAL is a multi-disciplinary open access archive for the deposit and dissemination of scientific research documents, whether they are published or not. The documents may come from teaching and research institutions in France or abroad, or from public or private research centers.

L'archive ouverte pluridisciplinaire **HAL**, est destinée au dépôt et à la diffusion de documents scientifiques de niveau recherche, publiés ou non, émanant des établissements d'enseignement et de recherche français ou étrangers, des laboratoires publics ou privés.

A refined sine finite element with transverse normal stress for thermoelastic analysis of laminated composite in cylindrical bending

P. Vidal^{a,*}, O. Polit^a

^a*LEME - EA 4416 - Université Paris Ouest
50 rue de Sèvres - 92410 Ville d'Avray - France*

Abstract

An unidimensional three-node composite finite element including the transverse normal effect is presented in the framework of the thermoelastic coupling. The kinematics is based on a sinus distribution with layer refinement and a second order expansion for the deflection. The calculation of the transverse normal stress comes from a weak formulation and takes into account the physical considerations. Numerical results for displacements and stresses are provided for very thick and thin structures in cylindrical bending. They are compared with exact elasticity solution and the results are promising.

Keywords: composite structures, transverse normal stress, finite element analysis, refined sine model.

1. INTRODUCTION

Composite and sandwich structures are widely used in the industrial field due to their excellent mechanical properties, especially their high specific stiffness and strength. In this context, they can be subjected to severe thermal conditions (through heating or cooling). For composite design, accurate knowledge of displacements and stresses is required. So, it is important to take into account effects of the transverse shear deformation due to the low ratio of transverse shear modulus to axial modulus, or failure due to delamination ... In fact, they can play an important role on the behavior of structures in services, which leads to evaluate precisely their influence on local stress fields in each layer, particularly on the interface between layers.

*Corresponding author

Email address: philippe.vidal@u-paris10.fr (P. Vidal)

The aim of this paper is to develop a finite element including the transverse normal deformation, so as to obtain accurate predictions for the behavior of laminated composite structures subjected to thermal loading. This analysis is limited to the elasticity area in relation to small displacements. In this context, it is necessary to take into account the transverse normal effect, in particular for thermal loads and thick structures.

According to published research, various theories in mechanics for composite or sandwich structures (beams and plates for the present scope) have been developed. Then, they have been extended to thermomechanical problems. The following classification is associated with the dependency on the number of unknowns with respect to the number of layers:

- the Equivalent Single Layer approach (ESL): the number of unknowns is independent of the number of layers, but continuity of transverse shear and normal stresses is often violated at layer interfaces. The first work for one-layer isotropic plates was proposed in [1]. Then, we can distinguish the classical laminate theory [2, 3] (it is based on the Euler-Bernoulli hypothesis and leads to inaccurate results for composites and moderately thick beams, because both transverse shear and normal strains are neglected), the first order shear deformation theory ([4]), and higher order theories.

In this family, some studies take into account transverse normal deformation. In the framework of thermomechanical problems, different approaches have been developed including mixed formulations [5] and displacement-based ones [6, 7, 8, 9].

- the Layerwise approach (LW): The number of dofs depends on the number of layers. This theory aims at overcoming the ESL shortcoming of allowing discontinuity of out-of-plane stresses on the interface layers. It was introduced in [10, 11]. For the thermomechanical analysis, readers can refer to [9] for displacement and [12, 13] for mixed approach.

In this framework, refined models have been developed in order to improve the accuracy of ESL models while avoiding the computational burden of the LW approach. Based on physical considerations and after some algebraic transformations, the number of unknowns becomes independent of the number of layers. [14] has extended the work of [15] for symmetric laminated composites with arbitrary orientation and a quadratic variation of the transverse stresses in each layer. A family of models, denoted zig-zag models, was employed in [16], then in [17, 18, 19]. More recently, it was

also modified and improved by some authors [12, 20] with different order of kinematics assumptions, taking into account the transverse normal strain.

Another way to improve the accuracy of the results consists in the sublaminates strategy, which is proposed in [21] and [22]. The number of subdivisions of the laminate thickness determines the accuracy of the approach. It allows to localize the layer refinement without increasing the order of approximation. Nevertheless, the computational cost increases with the number of numerical layers. For recent studies, the reader can also refer to [12, 23, 24].

This above literature deals with only some aspects of the broad research activity about models for layered structures and corresponding finite element formulations. An extensive assessment of different approaches has been made in [25, 26, 27, 28, 29].

In this work, an unidimensional three-node composite finite element is built for the thermomechanical coupling in cylindrical bending. This study aims at developing a low cost tool, efficient and simple to use. In fact, our approach is associated with the ESL theory. This element is totally free of shear locking and is based on a refined shear deformation theory [30] avoiding the use of shear correction factors for laminates. It is based on the sinus model [31] with the capability to include the transverse normal effect. In this work, the new important feature holds on an independent assumption introduced for the transverse normal stress. Then, a weak relation between the transverse normal strain deduced from the previous assumption and the derivative of the deflection is imposed in a least-square sense as in [5] for a {1,2}-order theory and [32, 33] for a {3,2}-order one. The transverse displacement is written under a second order expansion which avoids the Poisson locking mechanism (see [34]). For the in-plane displacement, the double superposition hypothesis from [35] is used: three local functions are added to the sinus model. Finally, the problem can be written under a displacement-based formulation, and this process yields to only eight independent generalized displacements. It should be noted that all interface and boundary conditions are exactly satisfied for displacements, transverse shear and normal stresses. Therefore, this approach takes into account physical meaning.

As far as the interpolation of this finite element is concerned, our element is C^0 -continuous except

for the transverse displacement associated with bending which is C^1 .

We now outline the remainder of this article. First the thermo-mechanical formulation for the present model is described. Then, the associated finite element is given. It is illustrated by numerical tests which have been performed upon various laminated structures in cylindrical bending. A parametric study is given to show the effects of different parameters such as length-to-thickness ratio and number of degrees of freedom. The accuracy of computations is also evaluated by comparison with an exact three-dimensional theory for laminates in bending [36, 37]. We put the emphasis on the direct calculation of the transverse shear and normal stresses. The results of our model is then compared with the approach consisting in calculating transverse shear and normal stresses from the equilibrium equations.

2. RESOLUTION OF THE THERMOMECHANICAL PROBLEM

2.1. The governing equations for thermomechanics

Let us consider a plate occupying the domain $\mathcal{B} = [0, L] \times [-\frac{h}{2} \leq z \leq \frac{h}{2}] \times [-\frac{b}{2} \leq x_2 \leq \frac{b}{2}]$ in a Cartesian coordinate (x_1, x_2, z) . The plate has an uniform cross section of height h , width b and is assumed to be straight. The structure is made of NC layers of different linearly elastic materials. Each layer may be assumed to be orthotropic in the plate axes. The plane (x_1, x_2) is the middle surface of the plate, and z is the transverse axis, see Fig. 1. This work is based upon a displacement approach for geometrically linear elastic plates.

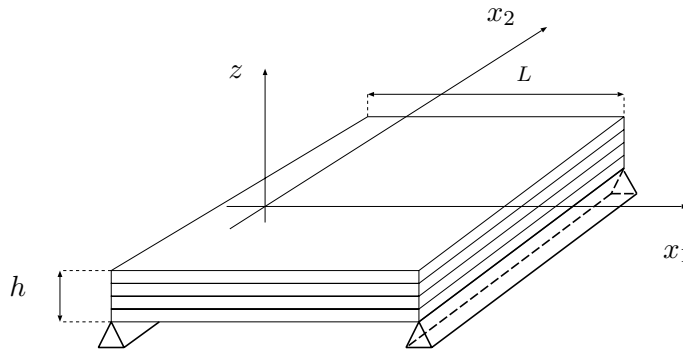


Figure 1: The laminated plate and co-ordinate system

The present study is limited to the cylindrical bending case. In the following, the x_2 direction is omitted.

2.1.1. Constitutive relation

Each layer of the laminate is assumed to be orthotropic. As precised previously, we suppose that $\varepsilon_{22}^{(k)} = \gamma_{12}^{(k)} = \gamma_{23}^{(k)} = 0$. Using matrix notation, the thermoelastic stress-strain law of the k^{th} layer can be written under a "mixed" form such as

$$\begin{bmatrix} \sigma_{11}^{(k)} \\ \varepsilon_{33}^{(k)} \\ \sigma_{13}^{(k)} \end{bmatrix} = \underbrace{\begin{bmatrix} \bar{C}_{11}^{(k)} & \bar{R}_{13}^{(k)} & 0 \\ -\bar{R}_{13}^{(k)} & \bar{S}_{33}^{(k)} & 0 \\ 0 & 0 & C_{55}^{(k)} \end{bmatrix}}_{[\bar{C}]} \begin{bmatrix} \varepsilon_{11}^{(k)} \\ \sigma_{33}^{(k)} \\ \gamma_{13}^{(k)} \end{bmatrix} - \underbrace{\begin{bmatrix} \alpha_{11}^{(k)} \bar{C}_{11}^{(k)} + \alpha_{22}^{(k)} \bar{C}_{12}^{(k)} \\ -\bar{R}_{13}^{(k)} \alpha_{11}^{(k)} - \bar{R}_{23}^{(k)} \alpha_{22}^{(k)} - \alpha_{33}^{(k)} \\ 0 \end{bmatrix}}_{[\bar{C}_{\Delta T}]} \Delta T(x_1, z) \quad (1)$$

$$\text{with } \bar{C}_{ij}^{(k)} = C_{ij}^{(k)} - \frac{C_{i3}^{(k)} C_{j3}^{(k)}}{C_{33}^{(k)}}, \bar{R}_{ij}^{(k)} = \frac{C_{ij}^{(k)}}{C_{33}^{(k)}}, \bar{S}_{33}^{(k)} = \frac{1}{C_{33}^{(k)}}.$$

In this expression, ΔT is the temperature rise, the C_{ij} are the three-dimensional stiffness coefficients and α_{ij} are the thermal expansion coefficients obtained after a transformation from the material axes to the Cartesian coordinate system.

The expression of $\Delta T(x_1, z)$ can be splitted into two parts such as $\Delta T(x_1, z) = G_{\Delta T}(z)F_{\Delta T}(x_1)$.

2.1.2. The weak form of the boundary value problem

Using the above matrix notation and for admissible virtual displacement $\vec{u}^* \in U^*$, the variational principle is this:

find \vec{u} in the space U of admissible displacements such that

$$-\int_{\mathcal{B}} [\varepsilon(\vec{u}^*)]^T [\sigma(\vec{u})] d\mathcal{B} + \int_{\mathcal{B}} [u^*]^T [f] d\mathcal{B} + \int_{\partial\mathcal{B}_F} [u^*]^T [F] d\partial\mathcal{B} = 0 \quad (2)$$

$$\forall \vec{u}^* \in U^*$$

where $[f]$ and $[F]$ are the prescribed body and surface forces applied on $\partial\mathcal{B}_F$. $\varepsilon(\vec{u}^*)$ is the virtual strain.

Eq. (2) is a classical starting point for finite element approximations.

2.2. The displacement field for the laminated structure in cylindrical bending

Based on the sinus function (see [30, 38]), a model which takes into account the transverse normal deformation is presented in this section. This refined sinus model includes a 2^{nd} order expansion for the transverse displacement.

It is based on both

- various works on beams, plates and shells, cf. references [38, 31, 30, 39, 40] concerning the refined theory,
- the so-called 1,2-3 double-superposition theory developed by Li and Liu [35],
- the particular treatment of the transverse normal stress developed in [32, 5].

It also follows works about local-global approach applied to thermomechanical analysis in [41]. This refined model (see [42, 43]) takes into account the continuity conditions between layers of the laminate for both displacements, transverse shear stress and transverse normal stress, and the free conditions on the upper and lower surfaces.

The kinematics of the model is assumed to be of the following particular form (with $w' = \partial w / \partial x_1$):

$$\begin{cases} u_1(x_1, z) = u(x_1) + z v_1(x_1) + z^2 v_2(x_1) + f(z)(\omega_3(x_1) + w_0(x_1)') \\ \quad + \sum_{k=1}^{NC} \left(\bar{u}_{loc}^{(k)}(x_1, z) + \hat{u}_{loc}^{(k)}(x_1, z) \right) (H(z - z_k) - H(z - z_{k+1})) \\ u_3(x_1, z) = w_0(x_1) + z w_1(x_1) + z^2 w_2(x_1) \end{cases} \quad (3)$$

where H is the Heaviside function defined by

$$\begin{cases} H(z - z_k) = 1 & \text{if } z \geq z_k \\ H(z - z_k) = 0 & \text{if not} \end{cases} \quad (4)$$

In the classic approach, w_0 is the bending deflection following the z direction, while u is associated with the membrane displacement of a point of the middle surface, and ω_3 is the shear bending rotation around the x_2 axis.

The local functions $\bar{u}_{loc}^{(k)}$ and $\hat{u}_{loc}^{(k)}$ based on the Legendre polynomial can be written as

$$\begin{cases} \bar{u}_{loc}^{(k)}(x_1, z) = \zeta_k u_{31}^k(x_1) + \left(-\frac{1}{2} + \frac{3\zeta_k^2}{2}\right) u_{32}^k(x_1) \\ \hat{u}_{loc}^{(k)}(x_1, z) = \left(-\frac{3\zeta_k}{2} + \frac{5\zeta_k^3}{2}\right) u_{33}^k(x_1) \end{cases} \quad (5)$$

where we have introduced the nondimensional coordinate $\zeta_k = a_k z - b_k$, with $a_k = \frac{2}{z_{k+1} - z_k}$ and $b_k = \frac{z_{k+1} + z_k}{z_{k+1} - z_k}$. The coordinate system is precised on Fig. 2.

In the context of the sinus model, we have $f(z) = \frac{h}{\pi} \sin \frac{\pi z}{h}$ and the derivative of this function will represent the transverse shear strain distribution due to bending.

Hence, it is not necessary to introduce transverse shear correction factors.

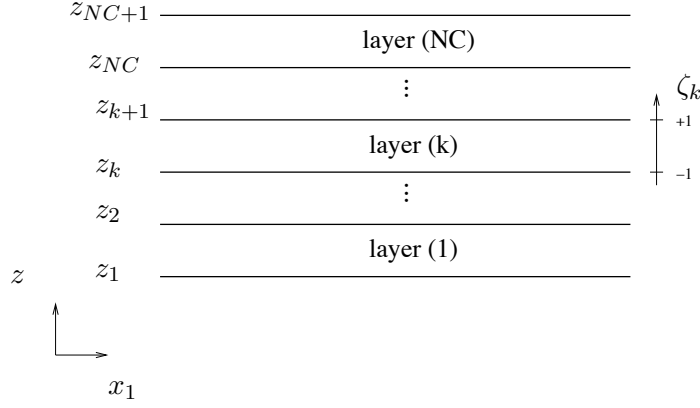


Figure 2: transverse coordinate of laminated plate

At this stage, $3 \times NC + 7$ generalized displacements are included in Eq. (3)-Eq. (5).

The following part is dedicated to the obtention of relations between kinematic unknowns from:

- lateral boundary conditions,
- interlaminar continuity conditions (in-plane displacement, transverse shear stress).

2.2.1. Continuity conditions and free conditions

From the displacement field Eq. (3), continuity conditions on the displacements and the interlaminar stress must be imposed:

- displacement continuity conditions at the interface layer k as in [44]:

$$\bar{u}_{loc}^{(k)}(x_1, z_k) = \bar{u}_{loc}^{(k-1)}(x_1, z_k) \quad k = 2, \dots, NC \quad (6)$$

$$\hat{u}_{loc}^{(k)}(x_1, z_k) = \hat{u}_{loc}^{(k-1)}(x_1, z_k) \quad k = 2, \dots, NC \quad (7)$$

- transverse shear stress continuity between two adjacent layers:

$$\sigma_{13}^{(k)}(x_1, z_k^+) = \sigma_{13}^{(k-1)}(x_1, z_k^-) \quad k = 2, \dots, NC \quad (8)$$

- free conditions of the transverse shear stress on the upper and lower surfaces

$$\sigma_{13}^{(1)}(x_1, z = -\frac{h}{2}) = 0 \quad \text{and} \quad \sigma_{13}^{(NC)}(x_1, z = \frac{h}{2}) = 0 \quad (9)$$

Finally, the number of generalized displacements is reduced to 8, which is independent of the number of layers. The remaining unknowns are u , w_0 , ω_3 , v_1 , v_2 , w_1 , w_2 and u_{31}^1 .

2.3. Expression of the strains and stresses

From Eq. (1), it is necessary to have the expressions of ε_{11} , γ_{13} and γ_{33} .

2.3.1. Expression of the strains

The in-plane and transverse shear strain can be deduced from the expression of the displacements (Eq. (3)) and the physical considerations given in Eq. (6), Eq. (7), Eq. (8) and Eq. (9):

$$\begin{aligned} \varepsilon_{11} = & u_{,1} + z v_{1,1} + (z^2 + S_\alpha(z)) v_{2,1} + (f(z) + S_\beta(z)) (w_{0,11} + \omega_{3,1}) \\ & + S_\delta(z) u_{31,1}^1 + S_\lambda(z) w_{1,11} + S_\mu(z) w_{2,11} + S_\eta(z) (w_{0,11} + v_{1,1}) \end{aligned} \quad (10)$$

$$\begin{aligned} \gamma_{13} = & \left(f(z)_{,3} + S_\beta(z)_{,3} \right) (w_{0,1} + \omega_3) + S_\delta(z)_{,3} u_{31}^1 + \left(1 + S_\eta(z)_{,3} \right) (w_{0,1} + v_1) \\ & + \left(2z + S_\alpha(z)_{,3} \right) v_2 + \left(z + S_\lambda(z)_{,3} \right) w_{1,1} + \left(z^2 + S_\mu(z)_{,3} \right) w_{2,1} \end{aligned}$$

The expressions of the continuity functions $S_\times(z)$ are given in Appendix A.

2.3.2. Expression of the transverse normal stress / strain

This section is dedicated to the deduced expression of the transverse normal strain from a particular form of the transverse normal stress. The process is based on some works developed in [32, 5] which introduce an independent polynomial expansion for the transverse normal stress.

In each layer (k), the transverse normal stress $\sigma_{33}^{(k)}$ is approximated by a quadratic expansion through the thickness as follows

$$\sigma_{33}^{(k)}(x_1, \zeta_k) = \sum_{i=0}^2 \sigma_{33i}^{(k)}(x_1) \zeta_k^i \quad (11)$$

The number of unknowns $\sigma_{33i}^{(k)}$ in $\sigma_{33}^{(k)}$, $k = 1, \dots, NC$ is reduced by imposing:

- the continuity of the transverse normal stress and its derivative at the layer interfaces,

- the free conditions on the top and bottom of the surface,
(At this stage, the number of unknowns is equal to NC)
- the conditions on the derivative of the transverse normal stress on the upper and lower surfaces for $NC > 3$.

Note that the number of remaining unknowns including in $\sigma_{33}^{(k)}$ must be greater than two so as to avoid a too more constrained problem.

Then, a weak relation is verified between the transverse normal strain and the derivative of the transverse displacement. It allows us to express the remaining unknowns in $\sigma_{33}^{(k)}$ with respect to the generalized unknowns of the present model that is :

$$\text{minimizing } \int_{-h/2}^{h/2} \left(\varepsilon_{33}^{(k)} - u_{3,z} \right)^2 dz \quad (12)$$

where the expression of $\varepsilon_{33}^{(k)}$ is given in Eq. (1).

This problem can be written under the form of a linear system. It allows us to deduce the expression of $\sigma_{33}^{(k)}$ with respect to the generalized unknowns and their derivatives u' , w_0'' , ω_3' , v_1' , v_2' , w_1 , w_2 , w_1'' , w_2'' and u_{31}' . This expression is given in Appendix B.

2.4. Matrix expression for the weak form

From the weak form of the boundary value problem Eq. (2), and using Eq. (C.1), Eq. (C.2) and Eq. (B.4), an integration throughout the cross-section is performed analytically in order to obtain an unidimensional formulation. Therefore, the first left term of Eq. (2) can be written under the following form:

$$\int_{\mathcal{B}} [\varepsilon(\vec{u}^*)]^T [\sigma(\vec{u})] d\mathcal{B} = \int_0^L [\mathcal{E}_s^*]^T [k] [\mathcal{E}_s] dx_1 - \int_0^L [\mathcal{E}_s^*]^T [f_{\Delta T}] dx_1 \quad (13)$$

where the matrix $[k]$ can be expressed as

$$[k] = \int_{\Omega} [F_s(z)]^T \begin{bmatrix} \bar{C}_{11}^{(k)} & 0 & 0 \\ 0 & \bar{S}_{33}^{(k)} & 0 \\ 0 & 0 & C_{55}^{(k)} \end{bmatrix} [F_s(z)] d\Omega$$

From the kinematics (see Eq. (3)), the generalized unknowns related to the transverse displacement $(w_i^h)_{i=0,2}$ must be C^1 -continuous ; whereas the rotation ω_3^h , the extension displacement u^h , v_1^h , v_2^h and u_{31}^1 can be only C^0 -continuous. Therefore, the generalized displacements $(w_i^h)_{i=0,2}$ are interpolated by the Hermite cubic functions $Nh_j(\xi)$.

According to the transverse shear locking phenomena, the other shear bending generalized displacement, rotation ω_3^h , is interpolated by Lagrange quadratic functions denoted $Nq_j(\xi)$. This choice allows the same order of interpolation for both $w_{0,1}^h$ and ω_3^h in the corresponding transverse shear strain components due to bending, thus avoiding transverse shear locking according to the field compatibility approach [45].

Finally, traction u^h , v_1^h , v_2^h and u_{31}^1 are interpolated by Lagrange quadratic functions.

2.5.3. Elementary matrices

In the previous section, all the finite element mechanical approximations were defined, and the elementary stiffness $[K_{uu}^e]$ matrix can be deduced from Eq. (13). It has the following expression:

$$[K_{uu}^e] = \int_{L_e} [B]^T [k] [B] dL_e \quad (15)$$

where $[B]$ is deduced from the relation between the generalized displacement vectors, see Eq. (C.1), and the elementary vector of degrees of freedom (d.o.f.) denoted $[q_e]$, i.e.:

$$[\mathcal{E}_s] = [B] [q_e] \quad (16)$$

The matrix $[B]$ contains only the derivatives of the interpolation functions and the Jacobian components.

The same technique can be used to define the elementary thermomechanical load vector, denoted $[B_{\Delta T}^e]$, but it is not detailed here.

3. Numerical results

In this section, the accuracy of the present theory is assessed on numerical tests performed upon various symmetric and unsymmetric laminated composite plates in cylindrical bending for a wide range of length-to-thickness ratios (from very thick to very thin structure). The results are compared with the exact 2D thermo-elasticity solution [37]. A special attention is also pointed toward the estimation of the transverse normal stress which has to be taken into account in this

coupled analysis. Note that the distribution of the transverse normal and shear stresses through the thickness is given from two approaches:

- a direct approach by using the constitutive relation for σ_{13} or the quadratic expansion for σ_{33} (Eq. (11)),
- a post-processing computation using the integration of the equilibrium equation (denoted Equil. Eq).

The problem is described as follows:

geometry: composite cross-ply plate, slenderness from $S=2$ to $S=100$; half of the structure is meshed. All layers have the same thickness.

boundary conditions: simply supported plate subjected to a temperature field as follows:

$$\Delta T(x_1, z) = T_{max} \frac{2z}{h} \sin\left(\frac{\pi x_1}{L}\right) \quad (17)$$

It corresponds to a cylindrical bending.

material properties:

$$\begin{aligned} E_L &= 172.4 \text{ GPa} , E_T = 6.895 \text{ GPa} , G_{LT} = 3.448 \text{ GPa} , \\ G_{TT} &= 1.379 \text{ GPa} , \nu_{LT} = \nu_{TT} = 0.25 \end{aligned}$$

where L refers to the fiber direction, T refers to the transverse direction.

$$\frac{\alpha_T}{\alpha_L} = 1125$$

where α_L, α_T are the thermal expansion coefficients in the fiber and normal direction respectively.

mesh: $N=8$

results: As in reference [13], we define the dimensionless quantities:

$$\begin{aligned} \bar{u} &= \frac{u_1}{\alpha_L T_{max} L} & \bar{w} &= \frac{hu_3}{\alpha_L T_{max} L^2} \\ \bar{\sigma}_{11} &= \frac{\sigma_{11}}{\alpha_L E_T T_{max}} & \bar{\sigma}_{13} &= \frac{\sigma_{13}}{\alpha_L E_T T_{max}} \end{aligned} \quad (18)$$

The exact results have been obtained from [36] and [37].

3.0.4. Properties of the finite element

Before proceeding to the detailed analysis, numerical computations are carried out for the rank of the element (spurious mode), convergence properties and the effect of aspect ratio (shear locking phenomenon).

The test is about simply supported moderately thick symmetric composite plates ($0^\circ/90^\circ/0^\circ/90^\circ/0^\circ$), as described above.

This element has a proper rank without any spurious energy modes when exact integration is applied to obtain the stiffness matrix (see [31]). In this purpose, a scheme with three integration points is used. There is also no need to use shear correction factors here, as the transverse strain is represented by a cosine function.

As far as the convergence property is concerned, Fig. 4 shows the evolution of the errors on the transverse displacement and the transverse shear stress with respect to the mesh size. It concerns moderately thick symmetric (5 layers) and unsymmetric (4 layers) lay-out. A very high convergence velocity can be emphasized whatever the stacking sequences. Based on progressive mesh refinement, a $N=8$ mesh is adequate to model the moderately thick laminated plate for a thermomechanical bending analysis. Moreover, the results obtained with coarse meshes are in good agreement with the reference values. The maximum error rate does not exceed 4%. Note also that this model gives very good results for the transverse shear stress calculated with the constitutive relation.

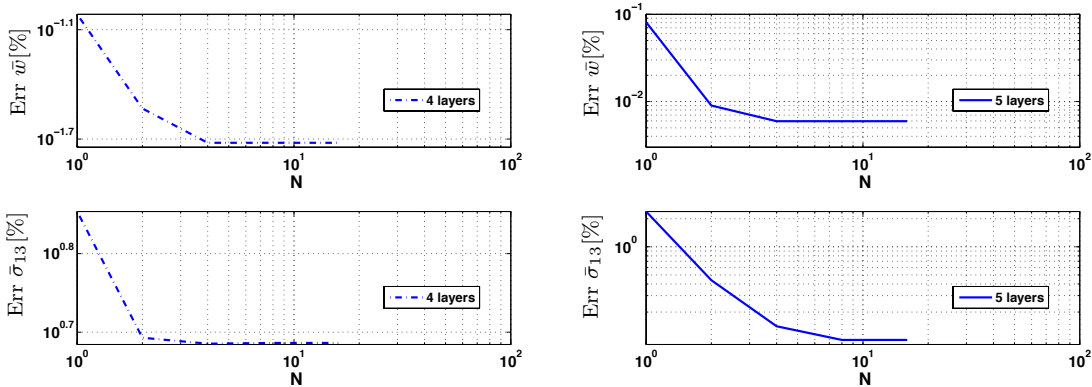


Figure 4: Error on $\bar{w}(L/2, h/2)$ and $\bar{\sigma}_{13}(0, 0)$ wrt the mesh size: mesh convergence study - 4/5 layers - $S=10$

Considering various values for aspect ratio, the normalized displacement obtained at the middle of the simply supported ($0^\circ/90^\circ/0^\circ/90^\circ/0^\circ$) composite plate is shown in Fig. 5 along with the exact

solution [37]. They are found to be in excellent agreement. It is also inferred from Fig. 5 that the present element is free from shear locking phenomenon as the element is developed using a field compatibility approach.

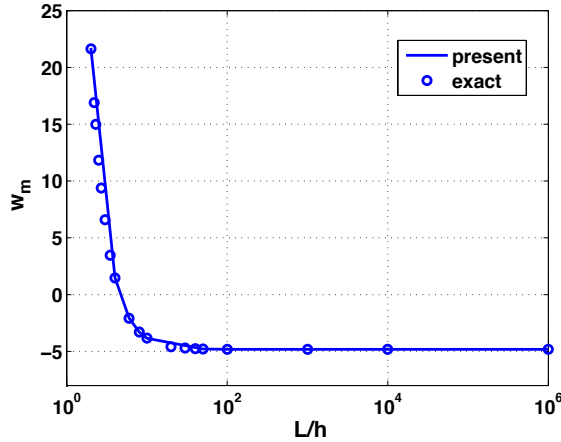


Figure 5: variation of the non-dimensional displacement ($w_m = u_3(L/2, 0)/(h\alpha_L T_{max} S^2)$) with respect to aspect ratio S - five layers ($0^\circ/90^\circ/0^\circ/90^\circ/0^\circ$); mesh $N=8$

3.1. Symmetric lay-out

A symmetric stacking sequence is considered to assess this finite element, namely five layers ($0^\circ/90^\circ/0^\circ/90^\circ/0^\circ$). The numerical results for the in-plane and transverse displacements, and for the in-plane and transverse shear stresses are given in Tab. 1 and Tab. 2. The slenderness ratio varies from $S=2$ to $S=100$. The very thick case $S=2$ is only given to show the limitation of the present theory. The transverse displacement is evaluated at the middle and at the top of the structure to show the non-constant variation through the thickness.

For the very severe case $S=2$, the error rate remains lower than 13 % for the stresses and 3 % for the displacements. Note that the deflection is very well estimated for all cases. The model has the capability to take into account the nonconstant variation through the thickness.

For $S \geq 4$, the results perform quite very well for thick as well as very thin plates. The maximum error rate is less than 1 %, except for the transverse shear stress where the error is more important for $S=4$ (5 %). Nevertheless, by considering the maximum value of the transverse shear stress located at $(0, \frac{-3h}{10})$, the error rate becomes less than 1 %.

For further comparison, Fig. 6 and Fig. 7 show the distribution of the in-plane, transverse

displacements and the in-plane, transverse shear stresses for $S=4$. Note that the evolution of these quantities along the thickness are similar for $S=10$. It is not given here. These quantities are quite close to the reference solution.

The transverse normal stress is presented in Fig. 8 only for the thick and very thick case where it plays the most important role. This quantity is directly calculated from the present theory or is issued from the equilibrium equation. The results are satisfactory, and particularly those obtained by the direct method. The free conditions on the upper and lower surfaces are fulfilled. No additional computational cost at the post-processing level is necessary.

S	$\bar{u}(0, h/2)$			$\bar{w}(L/2, 0)$			$\bar{w}(L/2, h/2)$		
	error	exact		error	exact		error	exact	
2	-15.6840	3 %	-15.2025	-21.7200	0.3 %	-21.6489	63.2250	2 %	64.6768
4	-9.9253	0.3 %	-9.8951	-1.4749	0.1 %	-1.4724	20.3167	0.2 %	20.3776
10	-7.9768	< 0.1 %	-7.9797	3.8466	< 0.1 %	3.8465	7.3523	< 0.1 %	7.3524
50	-7.5983	< 0.1 %	-7.5984	4.7880	< 0.1 %	4.7881	4.9284	< 0.1 %	4.9284
100	-7.5863	< 0.1 %	-7.5864	4.8173	< 0.1 %	4.8173	4.8524	< 0.1 %	4.8524

Table 1: $\bar{u}(0, h/2)$ and $\bar{w}(L/2, 0) / \bar{w}(L/2, h/2)$ for different values of S - 5 layers ($0^\circ/90^\circ/0^\circ/90^\circ/0^\circ$)

S	$\bar{\sigma}_{13}(0, 0)$			$\bar{\sigma}_{11}(L/2, -h/2)$		
	direct	error	exact	direct	error	exact
2	-62.8550	13 %	-72.8215	-931.85	4 %	-889.98
4	-31.0370	5 %	-32.7109	-476.97	1 %	-472.09
10	-12.4240	< 1 %	-12.4115	-323.06	< 1 %	-321.27
50	-2.4863	1 %	-2.4540	-293.16	< 1 %	-291.26
100	-1.2431	1 %	-1.2265	-292.21	< 1 %	-290.31

Table 2: $\bar{\sigma}_{13}(0, 0)$ and $\bar{\sigma}_{11}(L/2, -h/2)$ for different values of S - 5 layers ($0^\circ/90^\circ/0^\circ/90^\circ/0^\circ$)

3.2. Non-symmetrical lay-out

In this section, the results of a non-symmetrical four-layer laminated structure are presented. They are summarized in Tab. 3 and Tab. 4. For the very thick case, the error rate does not exceed 10 % for the stresses and 4 % for the displacements. The present theory can be used for a wide range of length-to-thickness ratios. For $S \geq 4$, the results are in good agreement with the exact solution. The error rate remains less than 1 % for the displacements and the in-plane stress. Note that the error rate associated to the local values of $\bar{\sigma}_{13}$ remain equal to 5 % for the thin case. But these results are local and it is more pertinent to complete these results with the distribution of this quantity through the thickness (See Fig. 9 left). The results perform quite well with respect to the

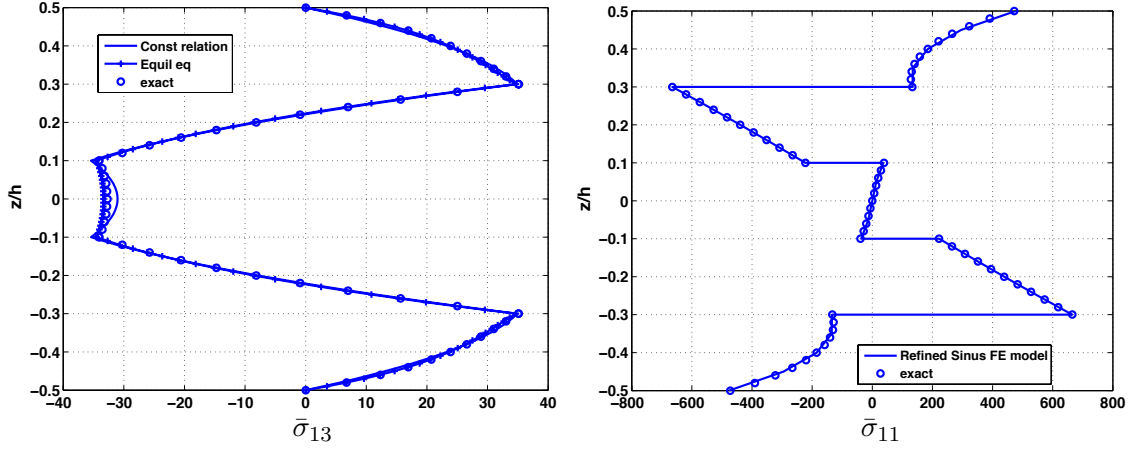


Figure 6: distribution of $\bar{\sigma}_{13}$ (left) and $\bar{\sigma}_{11}$ (right) along the thickness - S=4 - 5 layers

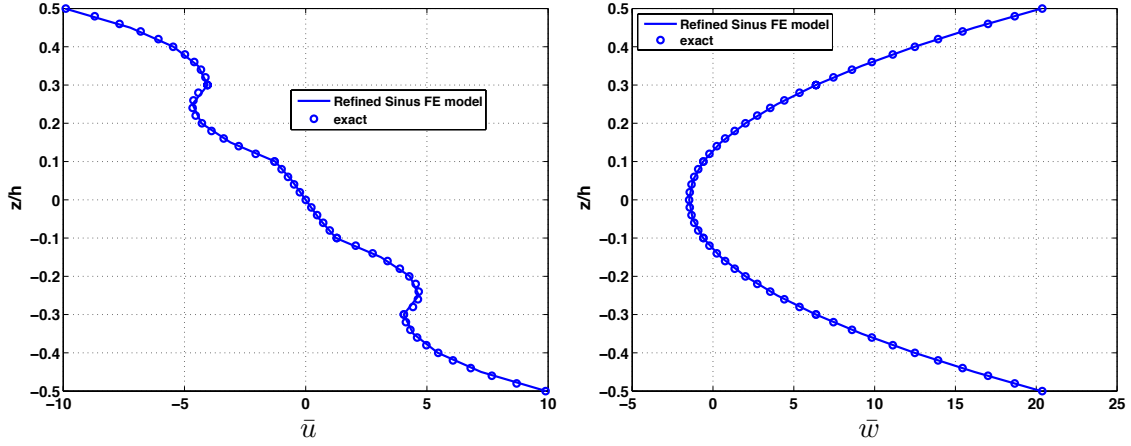


Figure 7: distribution of \bar{u} (left) and \bar{w} (right) along the thickness - S=4 - 5 layers

exact solution. The same remarks can be made for the distribution of the in-plane displacement, the deflection (Fig. 10), and the in-plane stress (Fig. 9) for the thick case. Given that the results related to the moderately thick case (S=10) have the same behavior as the thick case (S=4), they are not shown here as previously.

The estimation of the transverse normal stress given in Fig. 11 is also quite satisfactory for S=2 and S=4.

We notice that this test implies a complex behavior of the mechanical quantities through the thickness. A non-symmetric evolution is observed. The results obtained in the present approach proves the good efficiency of the model.

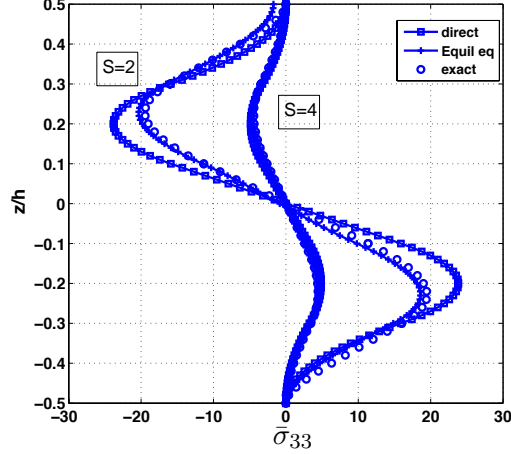


Figure 8: distribution of $\bar{\sigma}_{33}$ along the thickness - $S=2 / 4 - 5$ layers

S	$\bar{u}(0, h/2)$		$\bar{w}(L/2, 0)$		$\bar{w}(L/2, h/2)$				
	error	exact	error	exact	error	exact			
2	-158.4100	2 %	-155.0235	20.0745	0.04 %	20.0651	111.6550	4 %	106.9738
4	-73.0850	0.2 %	-72.8903	20.2873	0.04 %	20.2787	42.3050	1 %	41.8741
10	-38.3320	0.1 %	-38.3736	15.9000	0.02 %	15.9037	19.3520	< 0.1 %	19.3483
50	-31.0320	< 0.1 %	-31.0341	14.6492	< 0.01 %	14.6495	14.7868	< 0.1 %	14.7872
100	-30.7980	< 0.1 %	-30.7984	14.6070	< 0.01 %	14.6074	14.6420	< 0.1 %	14.6418

Table 3: $\bar{u}(0, h/2)$ and $\bar{w}(L/2, 0)$, $\bar{w}(L/2, h/2)$ for different values of S - 4 layers ($0^\circ/90^\circ/0^\circ/90^\circ$)

4. Conclusion

In this article, a refined finite element has been presented and evaluated through different benchmarks under thermomechanical loading. Special attention is pointed towards the transverse normal stress effect which plays an important role for thick structures and coupled problems. It is a unidimensional three-node multilayered finite element for static analysis with a parabolic distribution of the transverse displacement. Based on the sinus equivalent single layer model, a third order kinematic per layer is added, improving the bending description for thick structures. Moreover, an independent expression of the transverse normal stress is chosen. The transverse normal strain through the thickness is deduced by a weak formulation. This process based on a mixed approach allows us to formulate a classical displacement-based theory. It should be noted that all the interface and boundary conditions are exactly satisfied. So, this approach has a strong physical meaning and it allows us to get a number of unknowns independent of the number of

S	maximum of $\bar{\sigma}_{13}$			$\bar{\sigma}_{11}(L/2, -h/2)$		
	direct	error	exact	error	exact	exact
2	-186.710	10 %	-208.734	-1742.70	3 %	-1677.31
4	-134.880	0.3 %	-134.452	-1213.70	1 %	-1198.85
10	-61.9450	4 %	-59.0764	-950.79	< 1 %	-945.74
50	-12.7440	5 %	-12.0437	-890.42	< 1 %	-886.57
100	-6.3781	5 %	-6.0255	-888.46	< 1 %	-884.63

Table 4: maximum of $\bar{\sigma}_{13}$ and $\bar{\sigma}_{11}(L/2, -h/2)$ for different values of S - 4 layers ($0^\circ/90^\circ/0^\circ/90^\circ$)

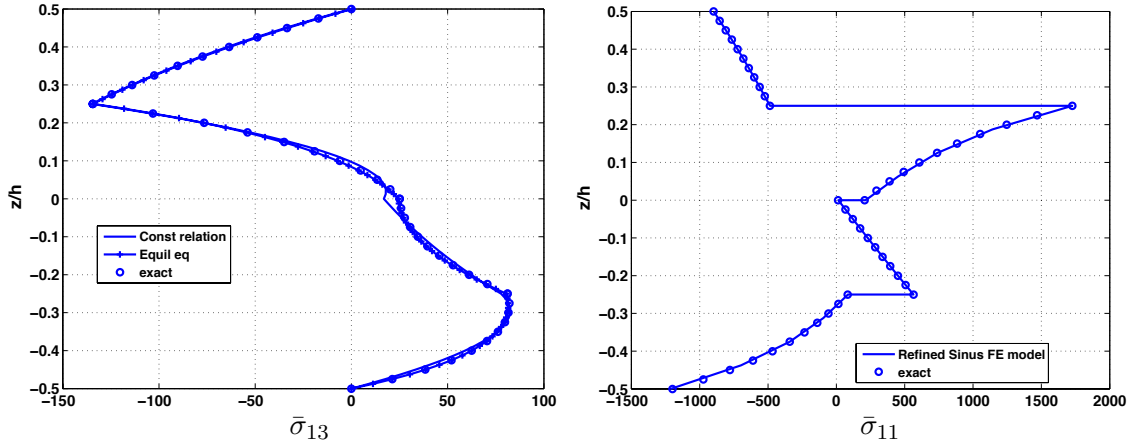


Figure 9: distribution of $\bar{\sigma}_{13}$ (left) and $\bar{\sigma}_{11}$ (right) along the thickness - S=4 - 4 layers

layers. Finally, there is no need for transverse shear correction factors.

Several numerical evaluations have proved that this model has very good properties in the field of finite elements. Convergence velocity is high and accurate results are obtained for very thick and thin cases. So, this finite element can be considered as a good compromise between accurate results and computational cost when compared to layerwise approach or plane elasticity model in commercial softwares. This approach allows to calculate the transverse shear and normal stresses directly with a satisfactory accuracy. The inclusion of the transverse normal stress is particularly important for thick structures and coupled thermo-mechanical problems.

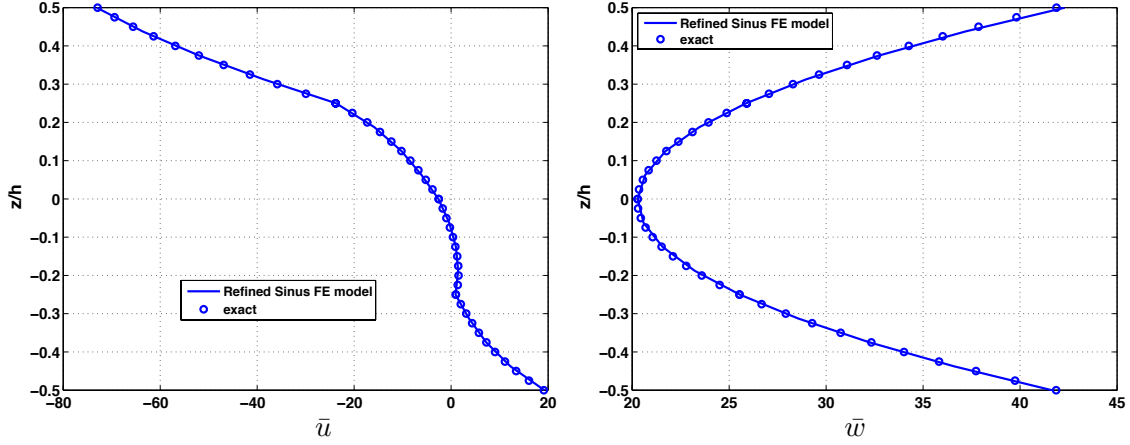


Figure 10: distribution of \bar{u} (left) and \bar{w} (right) along the thickness - S=4 - 4 layers

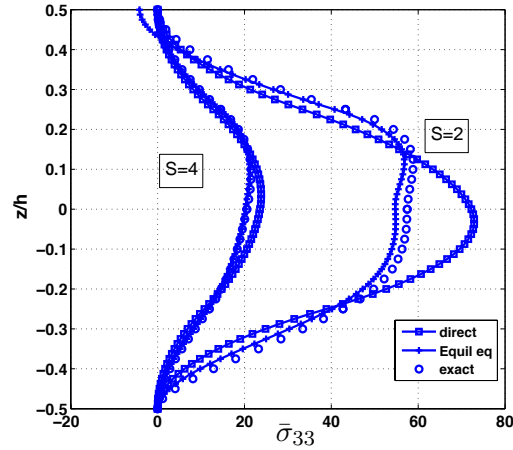


Figure 11: distribution of $\bar{\sigma}_{33}$ along the thickness - S=2/4 - 4 layers

Appendix A. Relation between the generalized displacements

Using the notations introduced in Eq. (3) and Eq. (5), the conditions Eq. (6)-Eq. (9) can be written under the following form:

$$\begin{aligned}
 [A]\{v\} &= \{b\}u_{31}^1(x_1) + \{c\}(\omega_3(x_1) + w_0(x_1)') + \{d\}(v_1(x_1) + w_0(x_1)') \\
 &\quad + \{e\}v_2(x_1) + \{f\}w_1(x_1)' + \{g\}w_2(x_1)'
 \end{aligned} \tag{A.1}$$

where $[A]$ is a $(3 * NC - 1) \times (3 * NC - 1)$ matrix,

$\{v\}^T = \{u_{32}^1 \ u_{33}^1 \ \dots \ u_{31}^j \ u_{32}^j \ u_{33}^j \ \dots \ u_{31}^{NC} \ u_{32}^{NC} \ u_{33}^{NC}\}^T$, and $\{b\}$, $\{c\}$, $\{d\}$, $\{e\}$, $\{f\}$, $\{g\}$ are vectors with $(3 * NC - 1)$ components.

From the resolution of this linear system, relations between $u_{31}^j (j \neq 1)$, u_{32}^j , u_{33}^j , $j = 1, \dots, NC$ and u_{31}^1 can be deduced. This relation can be written under the following form:

$$\begin{aligned} u_{3i}^j(x_1) &= \beta_i^j(\omega_3(x_1) + w_0(x_1)') + \eta_i^j(v_1(x_1) + w_0(x_1)') + \alpha_i^j v_2(x_1) \\ &\quad + \delta_i^j u_{31}^1(x_1) + \lambda_i^j w_1(x_1)' + \mu_i^j w_2(x_1)', \quad j = 1, \dots, NC \\ &\quad i = 1, 2, 3 \end{aligned} \tag{A.2}$$

$$\text{with } \delta_1^1 = 1, \alpha_1^1 = \beta_1^1 = \eta_1^1 = \lambda_1^1 = \mu_1^1 = 0$$

where α_i^j , β_i^j , δ_i^j , λ_i^j , μ_i^j , and η_i^j ($i = 1, 2, 3$) are the coefficients deduced from Eq. (A.1).

Finally, the 8 unknowns become u , w_0 , ω_3 , v_1 , v_2 , w_1 , w_2 and u_{31}^1 .

At this stage, the matrix notation can be easily defined using a generalized displacement vector as

$$[u]^T = [F_u(z)] [\mathcal{E}_u]$$

$$\text{with } [\mathcal{E}_u]^T = \left[u \quad w_0 \quad w_{0,1} \quad \omega_3 \quad u_{31}^1 \quad v_1 \quad v_2 \quad w_1 \quad w_{1,1} \quad w_2 \quad w_{2,1} \right] \tag{A.3}$$

and $[F_u(z)]$ depends on the normal coordinate z according to

$$[F_u(z)] = \begin{bmatrix} 1 & 0 & F_{u13}(z) & F_{u14}(z) & F_{u15}(z) & F_{u16}(z) & F_{u17}(z) & 0 & F_{u19}(z) & 0 & F_{u111}(z) \\ 0 & 1 & 0 & 0 & 0 & 0 & 0 & z & 0 & z^2 & 0 \end{bmatrix} \tag{A.4}$$

where

$$F_{u13}(z) = f(z) + S_\beta(z) + S_\eta(z)$$

$$F_{u14}(z) = f(z) + S_\beta(z)$$

$$F_{u15}(z) = S_\delta(z)$$

$$F_{u16}(z) = z + S_\eta(z)$$

$$F_{u17}(z) = z^2 + S_\alpha(z)$$

$$F_{u19}(z) = S_\lambda(z)$$

$$F_{u111}(z) = S_\mu(z)$$

and

$$S_\times(z) = \sum_{k=1}^{NC} \left(\zeta_k \times_1^k + \left(-\frac{1}{2} + \frac{3\zeta_k^2}{2}\right) \times_2^k + \left(-\frac{3\zeta_k}{2} + \frac{5\zeta_k^3}{2}\right) \times_3^k \right) \Delta H(k, k+1)$$

with $\times = \{\alpha, \beta, \delta, \eta, \lambda, \mu\}$ and $\Delta H(k, k+1) = H(z - z_k) - H(z - z_{k+1})$

Appendix B. Expression of the transverse normal stress

The following conditions are imposed for $\sigma_{33}^{(k)}$, $k = 1, \dots, NC$:

$$\begin{cases} \sigma_{33}^{(k-1)}(x_1, \zeta_{k-1} = 1) = \sigma_{33}^{(k)}(x_1, \zeta_k = -1) \\ \sigma_{33,z}^{(k-1)}(x_1, \zeta_{k-1} = 1) = \sigma_{33,z}^{(k)}(x_1, \zeta_k = -1) \end{cases} \quad (\text{B.1})$$

$$\begin{cases} \sigma_{33}^{(1)}(x_1, \zeta_1 = -1) = 0 \\ \sigma_{33}^{(NC)}(x_1, \zeta_{NC} = 1) = 0 \end{cases} \quad (\text{B.2})$$

for $NC > 3$,

$$\begin{cases} \sigma_{33,z}^{(1)}(x_1, \zeta_1 = -1) = 0 \\ \sigma_{33,z}^{(NC)}(x_1, \zeta_{NC} = 1) = 0 \end{cases} \quad (\text{B.3})$$

Using Eq. (B.1), Eq. (B.2), Eq. (B.3), and Eq. (12), the problem can be written under the form of a linear system. It allows us to deduce the expression of $\sigma_{33}^{(k)}$ with respect to the generalized unknowns and their derivatives u' , w_0'' , ω_3' , v_1' , v_2' , w_1 , w_2 , w_1'' , w_2'' and u_{31}^1 as

$$\begin{aligned} \sigma_{33}^{(k)}(x_1, \zeta_k) &= \Phi_u(\zeta_k)u'(x_1) + \Phi_{v_1}(\zeta_k)v_1'(x_1) + \Phi_{v_2}(\zeta_k)v_2'(x_1) + \Phi_{\omega_3}(\zeta_k)\omega_3'(x_1) \\ &+ \Phi_{u_{31}^1}(\zeta_k)u_{31}^1(x_1) + \Phi_{w_0}(\zeta_k)w_0''(x_1) + \Phi_{w_1}(\zeta_k)w_1(x_1) + \Phi_{w_2}(\zeta_k)w_2(x_1) \\ &+ \Phi_{w_1''}(\zeta_k)w_1''(x_1) + \Phi_{w_2''}(\zeta_k)w_2''(x_1) + \Phi_{\Delta T}(\zeta_k)F_{\Delta T}(x_1) \end{aligned} \quad (\text{B.4})$$

$\Phi_{\times}(\zeta_k)$ are the continuity functions. $\Phi_{\Delta T}(\zeta_k)$ is associated to the thermal term.

In this formulation, note that the transverse normal strain can be discontinuous at the interface between two adjacent layers (see Eq. (1) and Eq. (B.4)).

Appendix C. Matrix expression for the stress $\sigma_{33}^{(k)}$ and the strains ε_{11} , γ_{13}

The expressions Eq. (10) and Eq. (B.4) can be described using a matrix notation:

$$\begin{aligned} \begin{bmatrix} \varepsilon_{11}^{(k)} \\ \sigma_{33}^{(k)} \\ \gamma_{13}^{(k)} \end{bmatrix} &= [F_s(z)] [\mathcal{E}_s] + \begin{bmatrix} 0 \\ \Phi_{\Delta T}(\zeta_k)F_{\Delta T}(x_1) \\ 0 \end{bmatrix} \quad \text{with} \\ [\mathcal{E}_s]^T &= [u_{,1} \quad \vdots \quad w_{0,1} \quad w_{0,11} \quad \vdots \quad \omega_3 \quad \omega_{3,1} \quad \vdots \quad u_{31}^1 \quad u_{31,1}^1 \quad \vdots \quad v_1 \quad v_{1,1} \quad \vdots \\ &\quad v_2 \quad v_{2,1} \quad \vdots \quad w_1 \quad w_{1,1} \quad w_{1,11} \quad \vdots \quad w_2 \quad w_{2,1} \quad w_{2,11}] \end{aligned} \quad (\text{C.1})$$

and $[F_s(z)]$ depends on the normal coordinate z as

$$[F_s(z)] = \begin{bmatrix} 1 & 0 & f(z) + S_\beta(z) + S_\eta(z) & 0 & (f(z) + S_\beta(z)) & \dots \\ \Phi_u(\zeta_k) & 0 & \Phi_{w_0}(\zeta_k) & 0 & \Phi_{w_3}(\zeta_k) & \dots \\ 0 & 1 + (f(z)_{,3} + S_\beta(z)_{,3} + S_\eta(z)_{,3}) & 0 & (f(z)_{,3} + S_\beta(z)_{,3}) & 0 & \dots \\ 0 & S_\delta(z) & 0 & z + S_\eta(z) & 0 & z^2 + S_\alpha(z) & \dots \\ 0 & \Phi_{u_{31}}(\zeta_k) & 0 & \Phi_{v_1}(\zeta_k) & 0 & \Phi_{v_2}(\zeta_k) & \dots \\ S_\delta(z)_{,3} & 0 & 1 + S_\eta(z)_{,3} & 0 & 2z + S_\alpha(z)_{,3} & 0 & \dots \\ & & 0 & 0 & S_\lambda(z) & 0 & 0 & S_\mu(z) \\ & & \Phi_{w_1}(\zeta_k) & 0 & \Phi_{w_1'}(\zeta_k) & \Phi_{w_2}(\zeta_k) & 0 & \Phi_{w_2'}(\zeta_k) \\ & & 0 & z + S_\lambda(z)_{,3} & 0 & 0 & z^2 + S_\mu(z)_{,3} & 0 \end{bmatrix} \quad (C.2)$$

References

- [1] A. Basset, "On the extension and flexure of cylindrical and spherical thin elastic shells.," *Philos. Trans. Royal Soc. (London) Ser. A*, vol. 181, pp. 433–480, 1890.
- [2] Y. Tanigawa, H. Murakami, and Y. Ootao, "Transient thermal stress analysis of a laminated composite beam.," *J. Thermal Stresses*, vol. 12, pp. 25–39, 1989.
- [3] C. Wu and T. Tauchert, "Thermoelastic analysis of laminated plates. 1: Symmetric specially orthotropic laminates.," *J. Thermal Stresses*, vol. 3, no. 2, pp. 247–259, 1980.
- [4] R. Mindlin, "Influence of rotatory inertia and shear on flexural motions of isotropic, elastic plates.," *J. Applied Mech. ASME*, vol. 18, pp. 31–38, 1951.
- [5] A. Tessler, M. Annett, and G. Gendron, "A {1,2}-order plate theory accounting for three-dimensional thermoelastic deformations in thick composite and sandwich laminates.," *Compos. Struct.*, vol. 52, pp. 67–84, 2001.
- [6] J. Ali, K. Bhaskar, and T. Varadan, "A new theory for accurate thermal/mechanical flexural analysis of symmetric laminated plates.," *Compos. Struct.*, vol. 45, pp. 227–232, 1999.
- [7] K. Rohwer, R. Rolfes, and H. Sparr, "Higher-order theories for thermal stresses in layered plates.," *Int. J. Solids Struct.*, vol. 38, pp. 3673–3687, 2001.
- [8] R. Rolfes, A. Noor, and H. Sparr, "Evaluation of transverse thermal stresses in composite plates based on first-order shear deformation theory.," *Comput. Methods Appl. Mech. Eng.*, vol. 167, pp. 355–368, 1998.
- [9] A. Robaldo, "Finite element analysis of the influence of temperature profile on thermoelasticity of multilayered plates.," *Comput. Struct.*, vol. 84, pp. 1236–1246, 2006.
- [10] R. Heller and G. Swift, "Solutions for the multilayer timoshenko beam.," in *Report N VPI-E-71-12*, Virginia Polytechnic Institute, Blacksburg, VA, 1971.
- [11] G. Swift and R. Heller, "Layered beam analysis.," *J. Engng. Mech. ASCE*, vol. 100, pp. 267–282, 1974.
- [12] M. Gherlone and M. D. Sciuva, "Thermo-mechanics of undamaged and damaged multilayered composite plates: a sub-laminates finite approach.," *Comput. Struct.*, vol. 81, pp. 125–136, 2007.

- [13] E. Carrera, “An assessment of mixed and classical theories for the thermal stress analysis of orthotropic multilayered plates,,” *J. Thermal Stresses*, vol. 23, pp. 797–831, 2000.
- [14] J. Whitney, “The effect of transverse shear deformation in the bending of laminated plates,,” *J. Comp. Materials*, vol. 3, pp. 534–547, 1969.
- [15] S. Ambartsumyan, *Theory of anisotropic plates*. translated from russian by T. Cheron and Edited by J.E. Ashton, Technomic Publishing Co., 1969.
- [16] M. D. Sciuva, “Bending, vibration and buckling of simply supported thick multilayered orthotropic plates: an evaluation of a new displacement model,,” *J. Sound Vibr.*, vol. 105, pp. 425–442, 1986.
- [17] K. Bhaskar and T. Varadan, “Refinement of higher-order laminated plate theories,,” *AIAA J.*, vol. 27, pp. 1830–1, 1989.
- [18] C.-Y. Lee, D. Liu, and X. Lu, “Static and vibration analysis of laminated composite beams with an interlaminar shear stress continuity theory,” *Int. J. Num. Meth. Eng.*, vol. 33, pp. 409–424, 1992.
- [19] M. Cho and R. Parmerter, “Efficient higher-order composite plate theory for general lamination configurations,,” *AIAA J.*, vol. 31, pp. 1299–1306, 1993.
- [20] S. Kapuria, P. Dumir, and A. Ahmed, “An efficient higher order zigzag theory for composite and sandwich beams subjected to thermal loading,,” *Int. J. Solids Struct.*, vol. 40, pp. 6613–6631, 2003.
- [21] G. Flanagan, “A general sublaminar analysis method for determining strain energy release rates in composites,,” in *CP AIAA*, vol. 1994;94-1356, pp. 381–389, 1994.
- [22] R. Averill and Y. Yip, “Thick beam theory and finite element model with zig-zag sublaminar approximations,,” *AIAA J.*, vol. 34, no. 8, pp. 1627–1632, 1996.
- [23] U. Icardi, “Higher-order zig-zag model for analysis of thick composite beams with inclusion of transverse normal stress and sublaminar approximations,,” *Composite Part B : Eng. J.*, vol. 32, pp. 343–354, 2001.
- [24] M. Rao and Y. Desai, “Analytical solutions for vibrations of laminated and sandwich plates using mixed theory,,” *Compos. Struct.*, vol. 63, pp. 361–373, 2004.
- [25] A. Noor and W. Burton, “Assessment of computational models for multilayered composite shells,” *Appl. Mech. Rev.*, vol. 43, no. 4, pp. 67–97, 1990.
- [26] J. Reddy, “Mechanics of laminated composite plates - theory and analysis,,” CRC Press, Boca Raton, FL, 1997.
- [27] E. Carrera, “Theories and finite elements for multilayered, anisotropic, composite plates and shells,,” *Arch. Comput. Meth. Engng.*, vol. 9, pp. 87–140, 2002.
- [28] E. Carrera, “Historical review of zig-zag theories for multilayered plates and shells,,” *Appl. Mech. Rev.*, vol. 56, no. 3, pp. 287–308, 2003.
- [29] Y. Zhang and C. Yang, “Recent developments in finite elements analysis for laminated composite plates,,” *Compos. Struct.*, vol. 88, pp. 147–157, 2009.
- [30] M. Touratier, “An efficient standard plate theory,” *Int. J. Eng. Sci.*, vol. 29, pp. 901–916, 1991.
- [31] M. Ganapathi, B. Patel, O. Polit, and M. Touratier, “A c^1 finite element including transverse shear and torsion warping for rectangular sandwich beams,” *Int. J. Num. Meth. Eng.*, vol. 45, pp. 47–75, 1999.
- [32] G. Cook and A. Tessler, “A {3,2}-order bending theory for laminated composite and sandwich beams,,” *Composite Part B : Eng. J.*, vol. 29B, pp. 565–576, 1998.

- [33] A. Barut, E. Madenci, J. Heinrich, and A. Tessler, “Analysis of thick sandwich construction by a {3,2}-order theory,” *Int. J. Solids Struct.*, vol. 38, pp. 6063–6077, 2001.
- [34] E. Carrera and S. Brischetto, “Analysis of thickness locking in classical, refined and mixed multilayered plate theories,” *Compos. Struct.*, vol. 82, pp. 549–562, 2008.
- [35] X. Li and D. Liu, “Generalized laminate theories based on double superposition hypothesis,” *Int. J. Num. Meth. Eng.*, vol. 40, pp. 1197–1212, 1997.
- [36] N. Pagano, “Exact solutions for composite laminates in cylindrical bending,” *J. Comp. Materials*, vol. 3, pp. 398–411, 1969.
- [37] K. Bhaskar, T. Varadan, and J. Ali, “Thermoelastic solutions for orthotropic and anisotropic composite laminates,” *Composite Part B : Eng. J.*, vol. 27B, pp. 415–420, 1996.
- [38] O. Polit and M. Touratier, “A multilayered/sandwich triangular finite element applied to linear and nonlinear analysis,” *Compos. Struct.*, vol. 58, pp. 121–128, 2002.
- [39] P. Vidal and O. Polit, “A thermomechanical finite element for the analysis of rectangular laminated beams,” *Finite Elements in Analysis and Design*, vol. 42, no. 10, pp. 868–883, 2006.
- [40] P. Vidal and O. Polit, “Assessment of the refined sinus model for the non-linear analysis of composite beams,” *Compos. Struct.*, vol. 87, pp. 370–381, 2009. doi:10.1016/j.compstruct.2008.02.007.
- [41] W. Zhen, C. Wanji, and R. Xiaohui, “Refined global-local higher-order theory for angle-ply laminated plates under thermo-mechanical loads and finite element model,” *Comput. Struct.*, vol. 88, pp. 643–658, 2009.
- [42] P. Vidal and O. Polit, “A family of sinus finite elements for the analysis of rectangular laminated beams,” *Compos. Struct.*, vol. 84, pp. 56–72, 2008. doi:10.1016/j.compstruct.2007.06.009.
- [43] P. Vidal and O. Polit, “A refined sine-based finite element with transverse normal deformation for the analysis of laminated beams under thermomechanical loads,” *J. Mech. Mater. Struct.*, vol. 4, no. 6, pp. 1127–1155, 2009.
- [44] K. Sze, R. Chen, and Y. Cheung, “Finite element model with continuous transverse shear stress for composite laminates in cylindrical bending,” *Finite Elements in Analysis and Design*, vol. 31, pp. 153–164, 1998.
- [45] O. Polit, M. Touratier, and P. Lory, “A new eight-node quadrilateral shear-bending plate finite element,” *Int. J. Num. Meth. Eng.*, vol. 37, pp. 387–411, 1994.